

ORIGINAL ARTICLE

Celecoxib enhances apoptosis of the liver cancer cells via regulating ERK/JNK/P38 pathway

Zhe Jia*, Haitao Zhang*, Chao Ma, Ning Li, Menglong Wang

Department of General Surgery, Beijing YouAn Hospital, Capital Medical University, Beijing, China.

*Zhe Jia and Haitao Zhang contributed equally to this work.

Summary

Purpose: We aimed to investigate the effect of celecoxib on rats with liver cancer through the extracellular signal-regulated kinase (ERK)/c-Jun N-terminal kinase (JNK)/p38 pathway.

Methods: Sprague-Dawley rats (n=36) were divided into 3 groups (n=12 per group) randomly. In model group, the liver cancer model was established, and normal saline was intraperitoneally injected. In celecoxib group, the liver cancer model was also established, and celecoxib was intraperitoneally injected. After intervention for 30 d, the samples were taken. The body weight of rats was measured before modeling and before sampling. The morphology of liver tissues was observed via hematoxylin-eosin (HE) staining, the expressions of related proteins and messenger ribonucleic acids (mRNAs) were determined via Western blotting and quantitative polymerase chain reaction (qPCR), respectively, and the protein expressions of cysteinyl aspartate specific proteinase 3 (Caspase3) and Cyclin D1 in liver tissues were detected.

Results: Before modeling, there was no difference in the body weight of rats among groups. Before sampling, the body weight of rats was smaller in model group and celecoxib group than that in normal group, while it was larger in celecoxib group than that in model group. It was observed using HE staining that the morphology of liver tissues was normal in normal group, it was disordered, with a large number of tumor cells in model group, and it was a little disordered but improved in celecoxib group compared with that in model group. Furthermore, the protein expression of

phosphorylated ERK (p-ERK) significantly rose, while the relative protein expressions of p-JNK and p-p38 significantly declined in the other two groups compared with those in normal group. Compared with those in model group, the relative protein expression of p-ERK obviously declined, while the relative protein expressions of p-JNK and p-p38 obviously rose in celecoxib group. It was found via qPCR that the relative mRNA expression of Caspase3 was markedly lower, while that of Cyclin D1 was markedly higher in the other two groups than those in normal group. The relative mRNA expression of Caspase3 was markedly higher, while that of Cyclin D1 was markedly lower in celecoxib group than those in model group. In addition, according to the results of ELISA, the relative protein expression of Caspase3 greatly declined, while that of Cyclin D1 greatly rose in the other two groups compared with those in normal group. The relative protein expression of Caspase3 greatly rose, while that of Cyclin D1 greatly declined in celecoxib group compared with those in model group. Finally, the results of TUNEL assay showed that the apoptosis rate was remarkably decreased in the other two groups compared with that in normal group, while it was remarkably increased in celecoxib group compared with that in model group.

Conclusion: Celecoxib affects the apoptosis of liver cancer cells through regulating the ERK/JNK/p38 signaling pathway, thereby exerting an anti-tumor effect.

Key words: liver cancer, celecoxib, apoptosis, ERK/JNK/p38 signaling pathway.

Introduction

Liver cancer is a clinically common malignant tumor of the digestive system, whose morbidity and mortality rates are high, making it one of the

major tumors endangering human life and health [1,2]. According to the literature, the morbidity rate of liver cancer is relatively high in China. In par-

Corresponding author: Menglong Wang, MD. Department of General Surgery Center, Beijing YouAn Hospital, Capital Medical University, Fengtai District, 10 Xitoutiao, Beijing 100069, China.
Tel: +86 015835750808, Email: mlwangwangml@ccmu.edu.cn
Received: 28/03/2021; Accepted: 21/04/2021

ticular, viral hepatitis is one of the important causes of liver cancer in China, and the resulting liver cancer is also one of the major tumors leading to death of Chinese people. Therefore, it is extremely important to study the related pathogenesis and treatment methods of liver cancer.

Current studies [3-5] have shown that during the pathogenic process of liver cancer, excessive proliferation and insufficient apoptosis of liver cancer cells is one of the important causes of the development and deterioration of this disease. Therefore, effectively inhibiting the excessive proliferation and promoting the apoptosis of liver cancer cells in patients is considered as one of the important ideas for the treatment of liver cancer. The extracellular signal-regulated kinase (ERK)/c-Jun N-terminal kinase (JNK)/p38 signaling pathway is a key pathway in the body. Studies [6,7] have demonstrated that the ERK/JNK/p38 signaling pathway is closely related to cell proliferation and apoptosis, and plays a crucial regulatory role in cell proliferation and apoptosis. Therefore, the ERK/JNK/p38 signaling pathway is considered as an important entry point for the research on related mechanisms of liver cancer.

Celecoxib is a commonly used antipyretic and analgesic drug, and it has a good selective inhibitory effect on cyclooxygenase-2. According to recent studies [8,9], celecoxib exerts an excellent anti-tumor effect, but its related mechanism remains unclear. Therefore, the purpose of this study was to study the effect of celecoxib in rats with liver cancer through the ERK/JNK/p38 pathway.

Methods

Laboratory animals and grouping

A total of 36 Sprague-Dawley rats (200±20 g, 6-8 weeks) were divided into normal group (n=12), model group (n=12) and celecoxib group (n=12) using a random number table. They were adaptively fed with adequate food and water for 1 week. The Animal Ethics Committee of Capital Medical University Animal Center approved the present study.

Laboratory reagents and instruments

Celecoxib was provided by Pfizer Pharmaceuticals (Dalian, China), and primary antibodies against phosphorylated ERK (p-ERK), p-JNK and p-p38 antibodies and goat anti-rabbit secondary antibody were provided by Abcam (Cambridge, MA, USA). Hematoxylin-eosin (HE) staining kits, enzyme-linked immunosorbent assay (ELISA) kits and terminal deoxynucleotidyl transferase-mediated dUTP nick end labeling (TUNEL) assay kits were purchased from Boster (Wuhan, China), and quantitative polymerase chain reaction (qPCR) kits were purchased from Vazyme (Nanjing, China). A light microscope (Leica DMI 4000B/DFC425C) was obtained from Leica (Wetzlar,

Germany), a fluorescence qPCR instrument (ABI 7500, Applied Biosystems, Foster City, CA, USA) was obtained from Thermo Fisher Scientific (Waltham, MA, USA), and Image-Pro image analysis system was obtained from Bio-Rad (Hercules, CA, USA).

Modeling

The liver cancer model was established *via* injection of ascites containing Walker-256 liver cancer cell lines, specifically as follows: After anesthesia using 3% pentobarbital sodium solution (5 mL/kg) and disinfection, the abdominal cavity of rats was cut open to expose the liver in a supine position. Then the syringe was inserted obliquely into the liver tissues for about 0.5 cm to inject about 0.05 mL of cancerous ascites containing Walker-256 liver cancer cells (2×10^7 cells/mL). The bleeding point was pressed, and the abdominal cavity was closed and bandaged with sterile dressings.

Treatment in different groups

The rats underwent no treatment in normal group. In model group, the liver cancer model was established in the way described above, and an equal amount of normal saline was intraperitoneally injected every day after operation. In celecoxib group, the liver cancer model was also established in the way described above, and 0.2 mL of celecoxib solution (0.6mg/mL) was injected every day after operation. At 30 d after modeling, the samples were taken.

Weighing and sampling

The body weight of rats was measured and recorded before modeling and before sampling, and the changes in the body weight of each rat were compared and analyzed. After weighing, the samples were taken as follows: After successful anesthesia, 6 rats in each group were fixed with paraformaldehyde, and liver cancer tissues were taken and fixed in 4% paraformaldehyde at 4°C for 48 h. Then the paraffin sections were prepared for HE staining and TUNEL assay. Besides, the samples were directly taken from the remaining 6 rats in each group: Liver cancer tissues were taken and placed into Eppendorf (EP) tubes for Western blotting, ELISA and qPCR. RIPA reagent (Beyotime) was utilized to extract protein from tissues and cells.

HE Staining

The tissues were fixed up, baked and prepared into paraffin sections. The sections were soaked in xylene solution and gradient alcohol and routinely deparaffinized and hydrated, respectively. Then the sections were stained using HE staining kits, and the staining was observed under a microscope. The sections were mounted when the staining was clear.

Western blotting

Liver tissues were lysed with RIPA (Beyotime), and then the supernatant was quantified using the bicinchoninic acid (BCA) method (Beyotime, Shanghai, China). After protein denaturation, the protein was then separated using sodium dodecyl sulphate-polyacrylamide

gel electrophoresis (SDS-PAGE). Then the protein was transferred onto a polyvinylidene fluoride membrane (Millipore, Billerica, MA, USA), sealed with the TBST (25 mM Tris, 140 mM NaCl, and 0.1% Tween 20, pH 7.5) containing 5% skimmed milk for 1.5 h and incubated with the anti-p-ERK (1:1.000), anti-p-JNK (1:1.000) and anti-p-p38 primary antibodies (1:1.000) and secondary antibodies (1:1.000). After the membrane was washed with TBST, they were visualized using ECL reagents (Pierce, Rockford, IL, USA) and detected by ImageQuant LAS 4000 (Pittsburgh, PA, USA).

QPCR

Total RNA was extracted by using TRIzol reagent (Invitrogen, USA) and reversely transcribed into complementary DNA (cDNA) using the reverse transcription kit. The reaction system was 20 μ L in total, and the reaction conditions were as follows: reaction at 51°C for 2 min, pre-denaturation at 96°C for 10 min, denaturation at 96°C for 10 s, annealing at 60°C for 30 s, a total of 40 cycles. The relative expressions of related messenger RNAs (mRNAs) were detected, with glyceraldehyde-3-phosphate dehydrogenase (GAPDH) as an internal reference. The primer sequences are shown in Table 1.

ELISA

Abdominal aortic blood was centrifuged in a high-speed centrifuge at 14.000 g for 10 min, and the supernatant was harvested. The cell samples (1×10^5 cells) were prepared for the ELISA assay based on the protocol of the kits. At the end, a microplate reader was employed to measure the absorbance at 450 nm.

TUNEL assay

The sections were soaked in xylene solution and gradient alcohol for routine de-paraffinization and hydration, respectively. Then the sections were stained using TUNEL staining kits in the dark, mounted and observed under a fluorescence microscope.

Statistics

SPSS20.0 software (IBM, Armonk, NY, USA) was used for statistical analyses. Comparison between multiple groups was done using one-way ANOVA test followed by post hoc test (least significant difference). A p value < 0.05 was considered statistically significant.

Results

Comparison of body weight

As shown in Figure 1, before modeling, there was no difference in the body weight of rats among groups ($p > 0.05$). Before sampling, the body weight of rats was smaller in the model group and celecoxib group than that in the normal group ($p < 0.05$), while it was larger in the celecoxib group than that in the model group ($p < 0.05$).

HE staining results

The morphology of liver tissues was normal, hepatic lobules had intact and clear structure, and hepatocytes were arranged orderly without cell infiltration in the normal group. In the model group, the morphology of liver tissues was disordered, the structure of hepatic lobules was destroyed and disordered, and a large number of tumor cells could be seen (Figure 2). In the celecoxib group, the morphology of liver tissues was a little disordered but improved compared with that in the model group, the structure of hepatic lobules was destroyed, and some tumor cells could be seen.

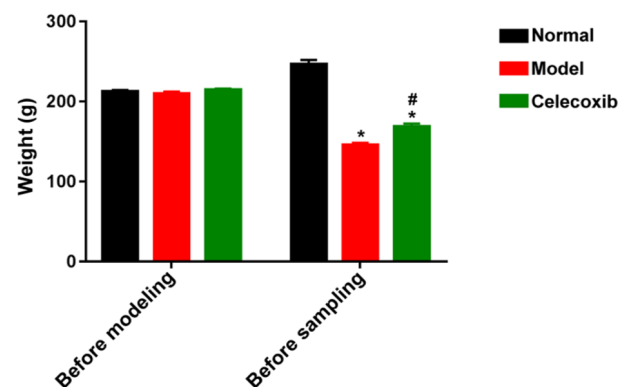


Figure 1. Comparison of body weight. Note: * $p < 0.05$ vs. normal group, # $p < 0.05$ vs. model group.

Table 1. Primer sequences

Gene	Primer sequence
CysteinyI aspartate specific proteinase 3 (Caspase3)	F: 5'-TCTTTCCAGATGAACAAATGGC-3' R: 5'-GCTGTTTTTCGCTTGAAATCTGC-3'
Cyclin D1	F: 5'-CTCCTCGCACTTCTGTTCCTC-3' R: 5'-CTCCTCGCACTTCTGTTCCTC-3'
GAPDH	F: 5'-ACGGCAAGTTCAACGGCACAG-3' R: 5'-GAAGACGCCAGTAGACTCCACGAC-3'

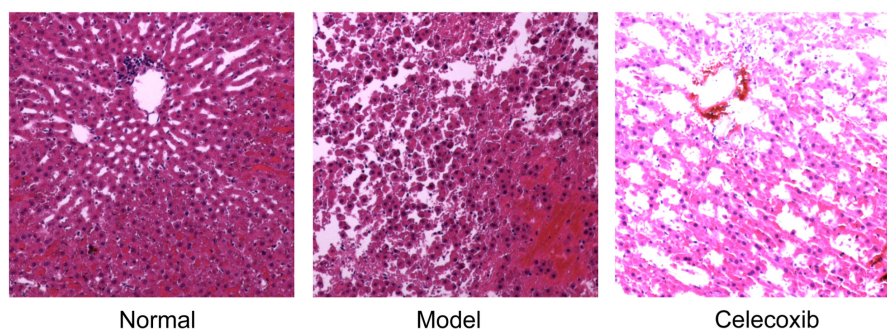


Figure 2. HE staining results (magnification: 200×).

Related protein expressions detected via western blotting

Normal group had a lower protein expression of p-ERK and higher protein expressions of p-JNK and p-p38, while the protein expressions of p-ERK, p-JNK and p-p38 were the opposite in the model group (Figure 3A). The assessment of protein expression was conducted with Image J software. According to the statistical results (Figure 3B), the relative protein expression of p-ERK significantly rose, while that of p-JNK and p-p38 significantly declined in the other two groups compared with those in the normal group ($p < 0.05$). Compared with those in the model group, the relative protein expression of p-ERK obviously declined, while that of p-JNK and p-p38 obviously rose in the celecoxib group ($p < 0.05$).

Related mRNA expressions detected via qPCR

The relative mRNA expression of Caspase3 was markedly lower, while that of Cyclin D1 was markedly higher in the other two groups than those in the normal group ($p < 0.05$). The relative mRNA expression of Caspase3 was markedly higher, while that of Cyclin D1 was markedly lower in the celecoxib group than those in the model group ($p < 0.05$) (Figure 4).

ELISA results

The relative protein expression of Caspase3 greatly declined, while that of Cyclin D1 greatly rose in the other two groups compared with those in the normal group ($p < 0.05$). The relative protein expression of Caspase3 greatly rose, while that of Cyclin D1 greatly declined in the celecoxib group compared with those in the model group ($p < 0.05$) (Figure 5).

TUNEL assay results

The number of apoptotic cells (green color) was larger in normal group, but smaller in the other two groups (Figure 6A). As shown in Figure

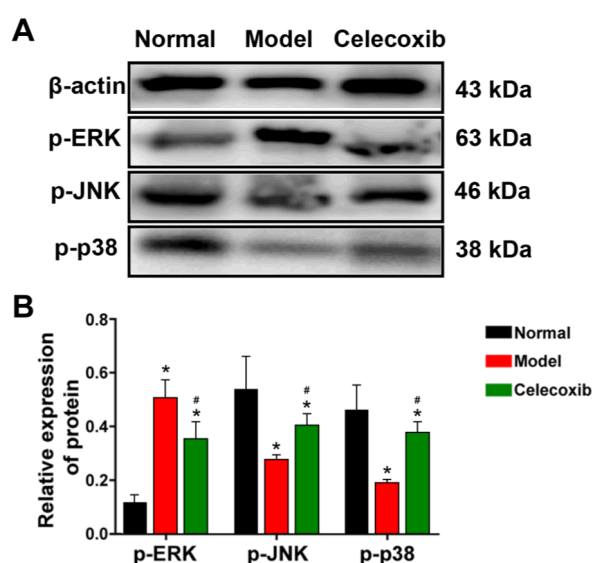


Figure 3. Related protein expressions detected via Western blotting. **A:** Western blotting bands, **B:** comparison of relative expressions of related proteins in each group. * $p < 0.05$ vs. normal group, # $p < 0.05$ vs. model group.

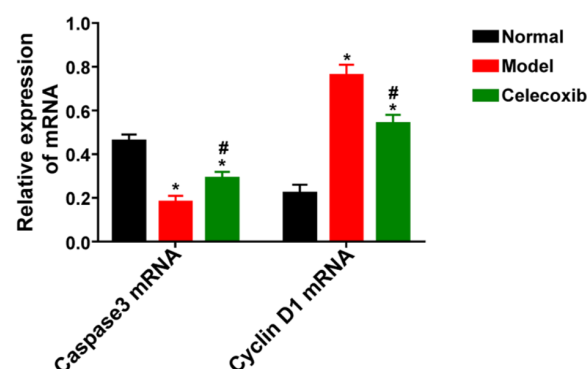


Figure 4. Related mRNA expressions. * $p < 0.05$ vs. normal group, # $p < 0.05$ vs. model group.

6B, the apoptosis rate was remarkably decreased in the other two groups compared with that in the normal group ($p < 0.05$), while it was remarkably increased in the celecoxib group compared with that in model group ($p < 0.05$).

Discussion

Liver cancer is a common malignant tumor of the digestive system in China, and it mainly leads to severe emaciation, abdominal distension, ascites, dull pain in the liver, jaundice, hepatomegaly and even cachexia, ultimately causing death of patients [10,11]. Liver cancer has high morbidity and mortality rates, and its mortality rate is second only to lung cancer and gastric cancer, seriously threatening the life and health of Chinese people. Liver cancer is characterized by insidious onset and rapid development, so the patients have often been in late stage when diagnosed. Studies have shown that hepatitis, including viral hepatitis and alcoholic hepatitis, is an important pathogenic factor of liver cancer. It is currently believed that the pathogenesis of liver cancer is complex and involves a variety of physio-pathological reactions and pathological mechanisms, including gene mutations, abnormalities of signal transduction pathways, cell proliferation and apoptosis [10-13]. At

present, surgical resection, chemoradiotherapy, interventional therapy and immunotherapy are dominating in the treatment of liver cancer, but there have been no ideal treatment methods yet. Therefore, it is of great importance to deeply study the related pathological mechanism of liver cancer and explore the related treatment methods based on this.

During the pathogenic process of liver cancer, excessive proliferation and low apoptosis level of liver cancer cells are the key factors to the occurrence and rapid development of liver cancer, and they are also the starting points for the effective inhibition on the development of liver cancer and its treatment. Studies have demonstrated that liver cancer cells have strong proliferation ability but apoptosis rarely occurs, which may be one of the important reasons for the rapid development of this disease [14-16]. Therefore, intervention based on these characteristics of liver cancer cells is a new idea for the treatment of liver cancer. The ERK/JNK/p38 signaling pathway plays an important regulatory role in the proliferation and apoptosis of liver cancer cells. It has been found that the phosphorylation levels of key molecules in the ERK/JNK/p38 signaling pathway (ERK, JNK and p38) have great changes in liver cancer tissues [17-19]. A large number of ERKs are phosphorylated to significantly increase their phosphorylation level, and then the massive expression of Cyclin D1 closely related to cell proliferation is promoted, thereby facilitating the proliferation of a large number of liver cancer cells. Meanwhile, the phosphorylation levels of JNK and p38 greatly decline, so that the expression of Caspase3 closely related to apoptosis is obviously decreased, thus making the apoptosis of liver cancer cells at a low level. In this study,

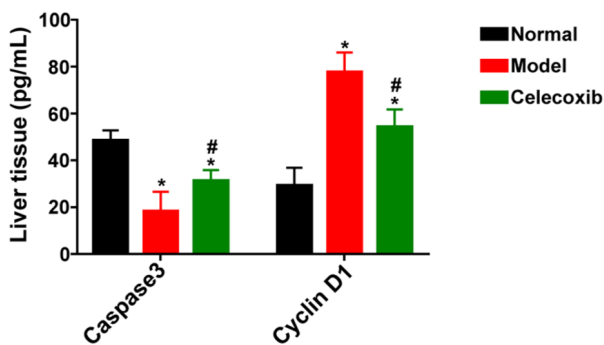


Figure 5. Protein expressions. * $p < 0.05$ vs. normal group, # $p < 0.05$ vs. model group.

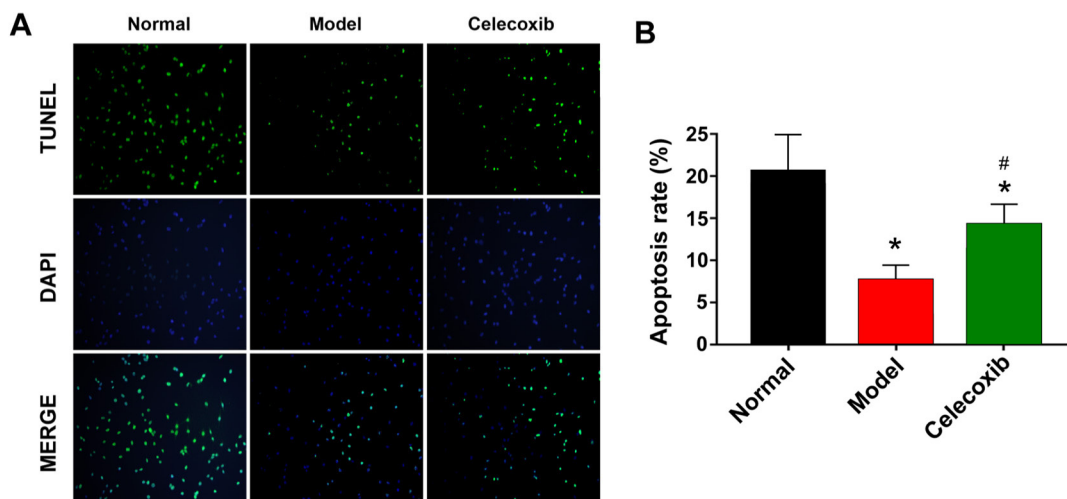


Figure 6. TUNEL apoptosis assay. **A:** TUNEL assay (magnification: 200×) **B:** comparison of apoptosis rate among all groups. * $p < 0.05$ vs. normal group, # $p < 0.05$ vs. model group.

the results further confirmed that the ERK/JNK/p38 signaling pathway had significant changes in liver cancer tissues, in which p-ERK had a markedly increased expression and p-JNK and p-p38 had markedly decreased expressions, consistent with the results of previous studies.

Celecoxib, one of the non-steroidal anti-inflammatory drugs, possesses a good antipyretic and analgesic effect, and it has been widely applied in the clinical treatment of muscle pain, inflammation, etc. A study has shown that celecoxib can better inhibit growth and promote apoptosis of tumor cells, thereby exerting a significant anti-tumor effect [20]. In this study, the findings confirmed that celecoxib could markedly inhibit the proliferation and promote the apoptosis of liver cancer cells, and improve the body weight of rats with liver cancer, thereby exerting a good anti-tumor effect. To study its related mechanism, the expressions of key molecules in the ERK/JNK/p38 signaling pathway

closely related to the proliferation and apoptosis of liver cancer cells were determined. The results showed that celecoxib could remarkably suppress the expression of p-ERK and promote the expressions of p-JNK and p-p38, thus enhancing the massive apoptosis of liver cancer cells. In conclusion, celecoxib affects the apoptosis of liver cancer cells through regulating the ERK/JNK/p38 signaling pathway, thereby exerting an anti-tumor effect.

Conclusions

In conclusion, celecoxib affects the apoptosis of liver cancer cells through regulating the ERK/JNK/p38 signaling pathway, thereby exerting an anti-tumor effect.

Conflict of interests

The authors declare no conflict of interests.

References

- Rodrigues RM, Kollipara L, Chaudhari U et al. Omics-based responses induced by bosentan in human hepatoma HepaRG cell cultures. *Arch Toxicol* 2018;92:1939-52.
- Markovic OT, Young DS, Markovic NS. Quinidine-induced decrease of intracellular esterase activity in a hepatoma cell line. *Clin Chem* 1988;34:512-7.
- Yen CJ, Ai YL, Tsai HW et al. Hepatitis B virus surface gene pre-S2 mutant as a high-risk serum marker for hepatoma recurrence after curative hepatic resection. *Hepatology* 2018;68:815-26.
- Chen LY, Huang YC, Huang ST et al. Domain swapping and SMYD1 interactions with the PWWP domain of human hepatoma-derived growth factor. *Sci Rep* 2018;8:287.
- Selvaraj P, Balasubramanian KA. Soluble forms of gamma-glutamyltransferase in human adult liver, fetal liver, and primary hepatoma compared. *Clin Chem* 1983;29:90-5.
- Li D, Dai C, Yang X, Li B, Xiao X, Tang S. GADD45a Regulates Olaparidox-Induced DNA Damage and S-Phase Arrest in Human Hepatoma G2 Cells via JNK/p38 Pathways. *Molecules* 2017;22
- Schliess F, Heinrich S, Haussinger D. Hyperosmotic induction of the mitogen-activated protein kinase phosphatase MKP-1 in H4IIE rat hepatoma cells. *Arch Biochem Biophys* 1998;351:35-40.
- Chu TH, Chan HH, Kuo HM et al. Celecoxib suppresses hepatoma stemness and progression by up-regulating PTEN. *Oncotarget* 2014;5:1475-90.
- Xu Z, Zhang M, Lv X, Xiang D, Zhang X, Chen L. The inhibitory effect of celecoxib on mouse hepatoma H22 cell line on the arachidonic acid metabolic pathway. *Biochem Cell Biol* 2010;88:603-9.
- Yang G, Bai Y, Wu X et al. Patulin induced ROS-dependent autophagic cell death in Human Hepatoma G2 cells. *Chem Biol Interact* 2018;288:24-31.
- Jiang Q, Sun Y, Guo Z et al. IL-23 enhances the malignant properties of hepatoma cells by attenuation of HNF4alpha. *Oncotarget* 2018;9:28309-21.
- Chen H, Yang X, Yu Z et al. Synthesis and biological evaluation of alpha-santonin derivatives as anti-hepatoma agents. *Eur J Med Chem* 2018;149:90-7.
- Liu S, Piao J, Liu Y et al. Radiosensitizing effects of different size bovine serum albumin-templated gold nanoparticles on H22 hepatoma-bearing mice. *Nanomedicine (Lond)* 2018;13:1371-83.
- Wang R, Fu T, You K et al. Identification of a TGF-beta-miR-195 positive feedback loop in hepatocytes and its deregulation in hepatoma cells. *Faseb J* 2018;32:3936-45.
- Wang H, Guo R, Du Z et al. Epigenetic Targeting of Granulin in Hepatoma Cells by Synthetic CRISPR dCas9 Epi-suppressors. *Mol Ther Nucleic Acids* 2018;11:23-33.
- Zhao C, Wang M, Liu Y, Liang Y, Han L, Chen C. Effects of the combination of As2O3 and AZT on proliferation inhibition and apoptosis induction of hepatoma HepG2 cells following silencing of Egr-1. *Onco Targets Ther* 2018;11:3293-301.
- Xu C, Shen G, Yuan X et al. ERK and JNK signaling pathways are involved in the regulation of activator protein 1 and cell death elicited by three isothiocyanates

- in human prostate cancer PC-3 cells. *Carcinogenesis* 2006;27:437-45.
18. Gschwantler-Kaulich D, Grunt TW, Muhr D, Wagner R, Kolbl H, Singer CF. HER Specific TKIs Exert Their Antineoplastic Effects on Breast Cancer Cell Lines through the Involvement of STAT5 and JNK. *PLoS One* 2016;11:e146311.
 19. El-Mas MM, Fan M, Abdel-Rahman AA. Role of rostral ventrolateral medullary ERK/JNK/p38 MAPK signaling in the pressor effects of ethanol and its oxidative product acetaldehyde. *Alcohol Clin Exp Res* 2013;37:1827-37.
 20. Shiyang M, Lei Y, Zhang L, Wang J. Research on the inhibiting effect of tan shinone IIA on colon cancer cell growth via Cox-2-Wnt/ β -catenin signaling pathway. *JBUON* 2018;23:1337-47.